3038–3044 Nucleic Acids Research, 1994, Vol. 22, No. 15

Tissue specific expression of the rat Ah-receptor and ARNT mRNAs

Lucy A.Carver, John B.Hogenesch and Christopher A.Bradfield*
Department of Molecular Pharmacology and Biological Chemistry and The Neuroscience Institute, Northwestern University Medical School, 303 E. Chicago Ave, Chicago, IL 60611, USA

Received May 9, 1994; Revised and Accepted July 6, 1994 GenBank accession nos U09000, U08986

ABSTRACT

The Ah-receptor (AHR) is a ligand activated transcription factor that mediates the biological effects of agonists such as 2,3,7,8-tetrachlorodibenzo-*p*-dioxin. Upon binding agonists, the AHR dimerizes with a structurally related protein known as ARNT and this heterodimer then binds cognate enhancer elements and activates the expression of target genes. In this report we describe the cloning of the rat AHR cDNA and a fragment of the rat ARNT cDNA for use as probes in ribonuclease protection analysis. Ribonuclease protection analysis indicated that the rat AHR mRNA is expressed at the highest levels in the lung > thymus > kidney > liver while lower levels were expressed in heart and spleen. The rat AHR and ARNT mRNAs were expressed in a largely coordinate manner across the eight tissues examined with the exception of the placenta where AHR levels were relatively low compared to ARNT. In these experiments, a rare splice variant of the AHR was cloned that encoded a protein with a deletion in the ligand binding domain. *In vitro* expression studies demonstrated that in contrast to the full length AHR, the splice variant did not bind ligand nor did it bind to a cognate enhancer element in the presence of ARNT.

INTRODUCTION

2,3,7,8-tetrachlorodibenzo-*p*-dioxin (TCDD) is the prototype for a number of highly toxic halogenated aromatic compounds (1). Exposure to TCDD can result in a variety of responses including porphyria, epithelial hyperplasia and metaplasia, cancer, liver damage, lymphoid involution and the induction of a number of enzymes involved in the metabolism of xenobiotics (1,2). Estimating the risk posed by the release of TCDD and related compounds into our environment is complicated by the fact that the sensitivity and pattern of toxicity can differ substantially among commonly used animal models (1,3). This variability in response to TCDD makes it difficult to identify appropriate animal models for studies directed at establishing safe human exposure levels (4).

Genetic and structure-activity studies indicate that most if not all of the biological responses elicited by TCDD are mediated through binding to a protein known as the Ah-receptor (AHR) (5–8). Current models of this signalling mechanism suggest that TCDD binds to an AHR-90 kilodalton heat shock protein (Hsp90) complex in the cytosol inducing a conformational change that leads to translocation of the complex to the nucleus (9–11,30). Once in the nucleus, the AHR then dimerizes with a structurally related protein known as the Ah-receptor nuclear translocator (ARNT) and the dimeric pair is then able to interact with dioxin responsive elements (DREs) upstream of regulated genes and activate their expression (8,12). Although there is considerable evidence indicating that this signalling pathway describes the mechanism by which TCDD elicits induction of the cytochrome P4501A1, 1A2, glutathione S-transferase Ya, and quinone reductase genes (13–16), the pathway leading to many other toxic responses such as tumor promotion and teratogenesis may be more complicated, or have additional features (1,2).

Our hypothesis is that all of the toxic effects of TCDD, that are relevant to human exposure, are the result of its binding to the AHR. As a corollary, we propose that different species' responses may arise from qualitative or quantitative differences in components of the AHR-ARNT signalling pathways. These differences may be related to differential AHR, ARNT, or Hsp90 function, tissue specific expression or differences in the spectrum of responsive genes. The AHR has been previously shown to exhibit a wide range of biochemical and structural variation between species (1, 3, 17–20). This has led us to characterize the molecular basis of this variation and begin to investigate the role it might play in differential signalling. To this end we wished to characterize differences in tissue distribution between the AHR and ARNT in a commonly used toxicological model, the rat. Not only should this information be valuable in understanding the organotropism of TCDD toxicity, but identification of tissues expressing either mRNA exclusively would suggest tissues where unique roles or partners for these proteins might exist.

MATERIALS AND METHODS

Oligonucleotide sequences

Oligonucleotide primer sequences are given below. Positions of oligonucleotides are depicted in Figure 1. Throughout the text, the notation human, murine or rat, indicates the sequence from which each oligonucleotide was designed.

*To whom correspondence should be addressed

OL52: 5′ CATCCTGGCATGGGAGCTAC 3′
OL72: 5′ GGTTCGAATTTCCAGGATGG 3′
OL77: 5′ GCCATGTCCATGTATCAGTGC 3′
OL79: 5′ GACTCGAGTCGACATCGATTTTTTTTTTTTTTTT 3′
OL102: 5′ AACATAAGGCACATAGCAAC 3′
OL107: 5′ CCGGTCGACAAGCCGGTGCAGAAAACAGTAAAGC 3′
OL108: 5′ CCGGTCGACCCCGCTGAAGGAATTAAGTCAAATCC 3′
OL109: 5′ CCGCTCGAGGTCGATGTCTTTGAAGTCAACCTCACC 3′
OL110: 5′ CCGCTCGAGTCTGACACAGCTGTTGCTGTGGCTCC 3′
OL122: 5′ CCCAAGCTTACGCGTGGTTCTCTGGAGGAAGCTGGTCTGG 3′
OL146: 5′ GAATTGTAATACGACTCACTATAGGG 3′
OL161: 5′ CCGACGCGTCGAGATCTCCAGCCCTTTCTCTCC 3′
OL176: 5′ CGGGATCCTTACACATTGGTGTTGGTACAGATGATGTACTC 3′
OL178: 5′ GCGGATCCACCATGGCCAGGGAAAATCACAGTG 3′

Cloning of the rat AHR

Our cloning strategy was to amplify the rat cDNA using polymerase chain reaction (PCR) primers directed against highly conserved regions of the human and murine cDNAs. To this end, first strand cDNA synthesis from 1.5 μg placental mRNA from a Fisher 344 rat (day 20 gestation) was carried out using an oligo-dT_{17} primer (OL79). One-tenth of this single stranded cDNA was used as a template in the first round of PCR containing 40 pmoles of primers OL107 and OL110 (Figure 1), 2.5 units *Taq* polymerase, 200 μM each dNTP, 10 mM Tris−HCl, 50 mM KCl, 1.5 mM $MgCl_2$, 0.001% gelatin (w/v) in a 100 μl reaction volume. The reaction conditions were 95°C for 5 min, after which the *Taq* polymerase was added at 72°C and the reaction continued for 35 cycles at 95°C 1 min, 65°C 1 min, 72°C 2 min plus a 3 sec/cycle extension followed by 72°C for 10 min. One microliter of this reaction was reamplified using the same conditions as above with the nested primers OL108 and OL109. To obtain a clone containing the stop codon and 3′ untranslated region (UTR), two successive PCRs were performed. Oligo dT_{17} primed first strand cDNA was made from 1.2 μg of liver mRNA from a pregnant female Fisher 344 rat. PCR was performed on 1/25 of this single stranded cDNA using the primers OL161 (a rat-specific primer located near the 3′ end of the initial rat AHR clone) and murine-specific primer OL52 (Figure 1). Reaction conditions were similar to those described above except for the following modification: 95°C 1 min, 58°C 1 min, 72°C 2 min for 35 cycles followed by 72°C 15 min. To obtain more downstream sequence, the rat liver cDNA was reamplified with OL77, a murine AHR primer, and OL102, a human AHR primer 801 bp downstream of the stop codon. Reactions were carried out as before except for the following change: 95°C 1 min, 52°C 1 min, 72°C 1.5 min for 35 cycles then 72°C for 15 minutes. The amplified fragments were subcloned into the pGEM-T vector (Promega, Madison, WI) and sequenced using the dideoxy chain termination method (21).

The 5′ region of the cDNA was amplified from a male Sprague Dawley liver cDNA library (Lambda-Zap II, Stratagene) using OL72 (a gene specific primer) and OL146 (a vector specific primer). The 50 μl PCR reaction contained 50 pmoles of each primer, 2 μl template (approximately 1×10^8 pfu/μl), 200 μM each dNTP, 2.5 units *Taq* polymerase, 10 mM Tris−HCl, 50 mM KCl, 0.001% gelatin, and 3 mM $MgCl_2$. Forty cycles were performed with the following conditions: 94°C 1 min, 55°C 1 min, and 72°C 1 min. Two and one-half microliters of these reactions were subsequently reamplified with a gene specific primer, OL122, and OL146. The reaction conditions were the same as above, except the annealing temperature was 60°C. The nested PCR products were analyzed on a 0.8% agarose gel, and verified by Southern analysis with a rat specific probe. Six of

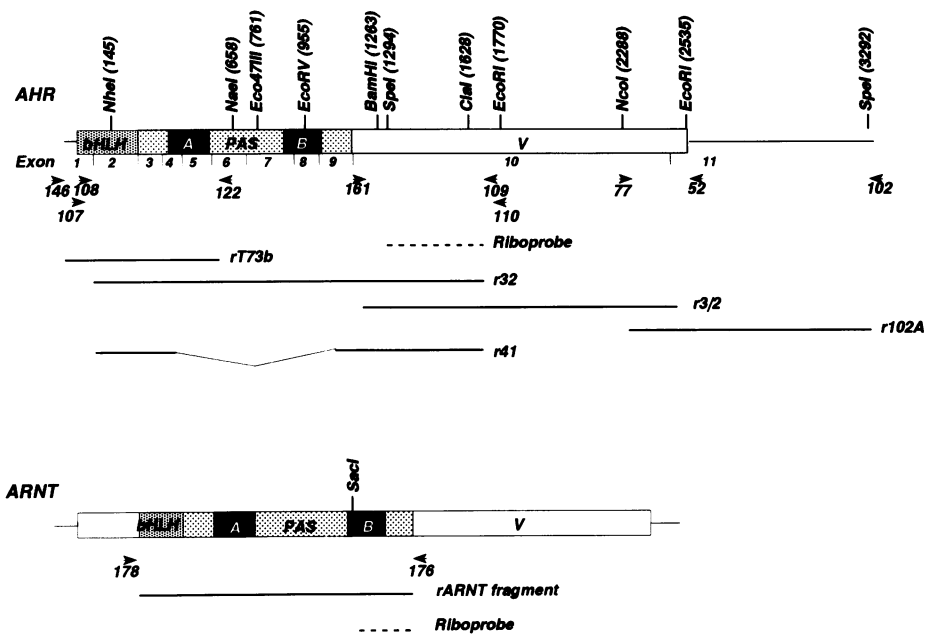

Figure 1. Location of PCR primers and cDNA clones of rat AHR and ARNT. Arrows: positions of oligonucleotide primers used in PCR for cloning the AHR and ARNT. Tips of the arrowheads indicate approximate positions of the primers. Exons: putative exon structure of the rat AHR as deduced from the murine structural gene (25). 'b': basic region. 'HLH': helix-loop-helix domain. 'PAS': PER-ARNT-AHR-SIM homology domain. 'A,B': A and B nucleotide repeats. 'V': variable domain. Dashed line: position of riboprobe used in the RPA. Top: Partial restriction map and location of PCR primers and rat AHR cDNA clones. Bottom: Location of PCR primers and rat ARNT fragment clone.

the clones greater than 500 bp were cloned into the pGEM-T vector and sequenced using the dideoxy chain termination method (21). One clone, T73b, contained nucleotides −16 to 639 (nucleotide sequences are numbered such that +1 corresponds to the A of the initiation methionine of the final rat AHR cDNA sequence). To obtain a continuous rat AHR cDNA, T73b was digested with *Pst*I/*Nhe*I. This fragment was cloned into a *Pst*I/*Nhe*I fragment of r32 and then cloned into the *Sac*I site of r3/2. This clone was designated rAHR and contained nucleotides −16 to 2557 of the rat AHR cDNA.

Cloning of a rat ARNT cDNA fragment

A rat ARNT cDNA fragment was obtained by amplification from the Sprague Dawley rat liver cDNA library described above. One μl of library (1×10^8 pfu/μl) was used as a template for PCR screening using human ARNT specific primers OL176 and OL178. Reaction conditions were the same as those for the AHR 5′ region PCR except 35 cycles of 94°C 1 min, 50°C 1 min, 72°C 1.5 min were carried out. The PCR products were electrophoresed on a 0.8% agarose gel, blotted to a nylon filter (Hybond N, Amersham, Arlington Heights, IL), probed with a random primed ^{32}P-labelled probe made to the 5′ 1106 bp of human ARNT, and autoradiographed (12). Several bands hybridized to the probe and a band of 1.1 kb, corresponding to the expected size of the rat ARNT fragment, was cloned into the pGEM-T vector and sequenced.

Ribonuclease protection analysis (RPA)

RPA was carried out using a 419 bp rat AHR cDNA probe corresponding to position 1294 to 1713 (Figure 1). Plasmid pr32 was linearized with *Spe*I and a riboprobe was synthesized by *in vitro* transcription using [α-^{32}P] UTP (800 Ci/mmole) and T7 RNA polymerase (22). The riboprobe (1×10^4 cpm) was added to 5 μg of rat liver total RNA and the assay was performed as described (23). We used an 80 bp riboprobe directed against the ribosomal 18S subunit as a loading control (pT7 RNA 18S, Ambion Inc., Austin TX). RPA on rat ARNT was carried out as above except that a 237 bp *Sac*I fragment from the rat ARNT cDNA was used as a template for riboprobe synthesis and 5×10^4 cpm of probe was used in the assay (Figure 1).

A

```
Rat          (   1)  M-SSGANITYASRKRRKPVQKTVKPVPAEGIKSNPSKRHRDRLNTELDRLASLLPFPQDVINKLDKLSVLRLSVTYLRAKSFFDVALKSTPADRSRGQDQ
Mouse (b-1)  (   1)  .-.....................I.....................................................................NG....
Human        (   1)  .N..S.....................I.....................................................S.............S.TE.NG...N

Rat          ( 100)  CRAQ-VRDWQDLQEGEFLLQALNGFVLVVTADALVFYASSTIQDYLGFQQSDVIHQSVYELIHTEDRAEFQRQLHWALNPSQCTDSAQGVDE-THGLPQP
Mouse (b-1)  ( 100)  ....-I.....................................................................----.........-A..P..A
Human        ( 101)  ...ANF.EGLN.....................T.....................................................E.G..IE.A.-....T

Rat          ( 198)  AVYYTPDQLPPENTA-FMERCFRCRLRCLLDNSSGFLAMNFQGRLKYLHGQNKKGKDGALLPPQLALFAIATPLQPPSILEIRTKNFIFRTKHKLDFTPI
Mouse (b-1)  ( 194)  .............-.S.....................................................................................
Human        ( 200)  V.C.N...I....SP-L.....I.....................K.......K......SI.....................................

Rat          ( 297)  GCDAKGQLI-LGYTEVELCNKGSGYQFIHAADMLHCAESHIRMIKTGESGMTVFRLLAKHSRWRWVQSNARLIYRNGRPDYIIATQRPLTDEEGREHLQK
Mouse (b-1)  ( 293)  .........-.........TR............I.....................................................................
Human        ( 299)  ......-R.V.....A...TR.............Y................I.....T.NN..T........L.K........V..........T...R.

Rat          ( 396)  RSMT-LPFMFATGEAVLYEISSPFSP-IMDPLPIRTKSN-TSRKDWAPQSTPSKDSFHPNSLMSALIQQDESIYLCPPSS---PAPLDSHFLMDSMSECG
Mouse (b-1)  ( 392)  ..-.S.....................-.............-.....................S.....................---..L.......G.V.K..
Human        ( 398)  .-N.K.....T........ATN..-.A......L...-.G..G..S.TT..L....LN.S..LA.MM........Y.A..TSST..FENN.FNE..N..R

Rat          ( 490)  SWQGSFAVA-SNEALLKHEEIRHTQDVNLTLSGGPSELFPDNKNNDLYSIMRNLGIDFEDIRSMQNEEFFRTDS--SGEVDFKDIDITDEILTYVQDSLN
Mouse (b-1)  ( 486)  ...D...A.G.-..A....Q.G.A.....A.....................................................TAA.....................
Human        ( 495)  N..DNT.PM-G.DTI....Q.DQP....-SFA..HPG..Q.S..S......K..........H....K...N.F--.......R...L............S

Rat          ( 587)  NSTLLNSACQQQPVSQHL-S-CMLQERLQLEQQQQLQQQHPTQTLEPQRQLCQVEV-PQHELGQKTKHMQVNGMFVSWNPAPPVSFSCPQQERKHICLLS
Mouse (b-1)  ( 585)  ..............T...-.-.................-..P.P.A....Q....-M.C..QD..--P..T.I..T.A....T.....N.....L..YQ.F.
Human        ( 591)  K.PFIP.DY...-Q.LA.N.S..V..H.H..---.-....------H.K.-VV..-...QQ.C..M.........EN..SNQF.P.N....DPQQYNVFT

Rat          ( 684)  GLQGTAQEFPYKSEVDSMPYTQNFAPCNQSLLPEHSKGTQLDFPGRDFERSLHPNVSNLEEFVSCLQVPENQRHGINSQSAMVSPQAYYAGAMSMYQCQA
Mouse (b-1)  ( 679)  S...........P....V...........P........SV..........P....TT...-D...........S.........................P
Human        ( 677)  D.H.IS........M.........IS...PV..Q...C.E..Y.MGS..P.PY.TT.S..D..T...L....K..L.P...IIT..TC....V......P

Rat          ( 784)  GPQDTPVDQMQYSPEIPGSQAFLSKFQSPSILNEAYSADLSSIGHLQTAAHL-PRLA---EAQPLPDITPSGFL*
Mouse (b-1)  ( 778)  ...R.....T...S...........V*
Human        ( 777)  E..H.H.G....N.VL..Q....N...-NGV...T.P.E.NN.NNT..TT..Q.-.HHPS..R.F..L.S....*
```

B

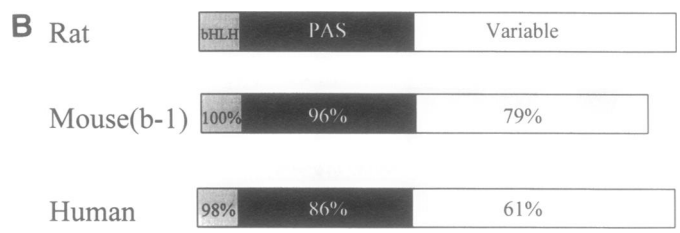

Figure 2. Comparison of the rat, mouse and human AHRs. **A.** Comparison of the amino acid sequences of the rat, murine, and human AHRs. Only the amino acids that differ from the rat AHR are shown. Dotted line indicates identity while dashed lines indicate gaps inserted to improve alignment. Asterisk denotes location of stop codon. Allele of murine AHR is indicated in parenthesis. **B.** Figure showing amino acid identity between the bHLH, PAS, and variable domains of the rat, murine (27), and human (26) AHRs.

In vitro expression

In vitro expression of the rAHR was carried out as previously reported using TNT-coupled rabbit reticulocyte lysate (Promega) (24). In a 50 μl reaction 1 μg of plasmid DNA containing the full length rat AHR cDNA was added to 25 μl rabbit reticulocyte lysate (Promega), 20 μM complete amino acid mixture, 40 units of RNAse inhibitor and 1 unit SP6 RNA polymerase. The reaction was carried out for 2 hrs at 30°C, and the mixture was either used immediately for analysis or kept frozen at −80°C for future use. The receptor was also labelled with [^{35}S]methionine using this system and subjected to sodium dodecyl sulfate polyacrylamide gel electrophoresis (SDS-PAGE) for molecular weight analysis and quantitation.

Photoaffinity labelling and gel shift assay

Photoaffinity labelling and gel-shift analysis were carried out as previously reported with *in vitro* translated receptor (24).

RESULTS AND DISCUSSION

Cloning of the rat AHR

Using highly conserved regions between the human and murine AHR cDNAs, we designed a series of primers to amplify the entire open reading frame (ORF) of the rat cDNA from total RNA and cDNA libraries. Since the structural gene of the murine AHR has been cloned previously (25), we used its intron-exon pattern as an additional guide to design primers that would maximize our chances of isolating splice variants (Figure 1). Using primers that spanned the basic helix-loop-helix (bHLH) and PER-ARNT-AHR-SIM (PAS) homology domain, two major products were identified, cloned, and sequenced. Clone r32 contained a 1.6 kb ORF corresponding to the similar region in the human and mouse receptor. The splice variant, r41, was 0.94 kb and contained a continuous ORF with a deletion of 699 bp (corresponding to nucleotides 430 to 1129). A comparison with the murine structural gene suggested that these variants are missing exons 5 through 9 which contain the ligand binding domain, the putative Hsp90 binding domain, and most of the PAS domain (24,25,30). To complete the 3′ end of the clone through the stop codon, we used two successive PCR reactions using primers made to homologous regions in the mouse and human 3′ ends to amplify the corresponding region of the rat AHR (Figure 1). The two clones obtained, r3/2 and r102A, together contained nucleotides 1486 to 3343 with an in-frame stop codon at position 2560. Since these clones allowed us to deduce the complete ORF, we did not attempt to obtain the polyadenylation sequence. To obtain a 5′ sequence of the cDNA that included the initiation methionine, we screened a Sprague Dawley rat liver cDNA library by PCR and isolated 6 separate species above 500 bp. These were sequenced and the largest clone, rT73b, was found to contain nucleotides −16 to 639 (Figure 1). Although we were not able to isolate a clone containing an upstream, in-frame stop codon, the initiation methionine identified does conform to a consensus translational start site and is homologous to the start site for the AHR cloned from the mouse and human (26−28). To generate clones that would express both the full length AHR and the splice variant, the PCR fragments were joined into a continuous cDNA from nucleotides −16 to 2560 and cloned downstream of the SP6 promoter in the vector pGEM-T. The full length AHR was then designated rAHR and the splice variant was named rAHR/Δ142−376 to denote the missing amino acids.

Comparison of the rat, human, and mouse AHR

The amino acid sequences encoded by the human, murine, and rat AHR cDNAs were compared using the PALIGN program (29) (Figure 2A). This analysis revealed a high degree of conservation in the amino terminal half of the receptor with 100% identity between the rat and mouse receptors and 98% between the rat and human receptors in the bHLH domain (Figure 2B). The amino acid identity in the PAS domain between the rat and mouse was 96% but only 86% between the rat and human receptors. This high degree of homology is not surprising since these domains are thought to mediate DNA binding, ARNT and Hsp 90 interaction, and ligand binding functions (24, 30, 31). The C-termini of the deduced protein sequence is not as well conserved between the three species at the amino acid level with an 79% identity between rat and mouse and only 61% between rat and human. This poorly conserved region has been referred to previously as a variable domain (25).

Generation of a rat ARNT partial cDNA clone

To compare the tissue-specific expression levels of the AHR and ARNT by RPA it was necessary to clone a fragment of the rat ARNT cDNA to generate a corresponding riboprobe. To this end, the Sprague Dawley rat liver library was screened by PCR using ARNT specific primers made to the bHLH and PAS domains of human ARNT (Figure 1). Since these domains are thought to be involved in AHR dimerization and DNA binding, we presumed that they would be highly homologous between the two species and primers made in these areas would have the highest chance of annealing specifically to rat ARNT sequences contained in the library. Using this strategy, a product of 1150 nucleotides was identified as rat ARNT by Southern blot analysis and was cloned and sequenced. This clone, rARNT-bHLH/PAS, contained a continuous ORF corresponding to the region between nucleotides 268 and 1392 of the human ARNT (12). These two clones share a 98% amino acid identity in this region indicating that the clone is in fact a fragment of the rat ARNT.

RPA of the rat AHR and ARNT

RPA of total RNA from eight different female Fisher 344 rat tissues was carried out using a 419 bp riboprobe generated from a region common to both the full length AHR and the splice variants (Figure 1). This probe detected the presence of a single species in all tissues with lung, thymus, liver, and kidney containing the highest levels of expression and heart and spleen showing the lowest (Figure 3A, C). These levels are in agreement with those reported previously using ^{3}H-TCDD binding as the method of AHR protein quantitation (20, 32). The high level of correlation between mRNA levels as measured by RPA and the amount of protein as deduced by the number of binding sites attests to the accuracy of RPA as a method to determine expression levels of AHR in tissues.

To determine the relative expression of the splice variant, rAHR/Δ142−376, the RPA was repeated using a probe which would detect both this variant and the full length rAHR. The probe detected only a single species corresponding to the larger AHR clone and showed levels of expression identical to those observed with the first probe (data not shown). Although we could consistently amplify this variant from placental tissue, we could not detect its presence by RPA of any of the tissues, suggesting that this transcript is expressed at very low levels and may be of little biological consequence.

Initially, we chose to use placental cDNA as a template for PCR. This decision was based on our earlier expression data from the human AHR that suggested that the highest level of human AHR mRNA was in human placental tissue (26). However, comparison of the data from the RPA of rat tissues to that obtained from northern analysis of human tissues indicate that the tissue-specific expression of the AHR between the two species differs significantly (26). The AHR seems to be expressed at relatively high levels in human placenta, at term, while in the rat placenta taken at 16 days AHR expression appears to be low relative to other tissues. The significance of this finding is difficult to assess because of the unique physiologies and the differences in gestation time between rat and human placenta. Given our validation of these reagents as probes of AHR and ARNT expression, we plan to re-examine this pattern of expression at a developmental and cellular level using *in situ* hybridization.

We were interested in comparing the tissue distribution of the AHR with that of its partner, ARNT, to see if there were any variations in the relative levels of their mRNA expression. It was our hypothesis that if these two proteins act only in concert, then their relative expressions across tissue should be coordinated. Lack of coordination might suggest additional biological roles for these proteins or identify tissues where unique partners might be present. Using a 237 bp fragment of the rat ARNT cDNA to probe the same tissues as the AHR (Figure 1), we found that the AHR and ARNT are expressed in a relatively coordinate manner across the eight tissues examined (Figure 3D). A single species corresponding to the rat ARNT mRNA was detected in

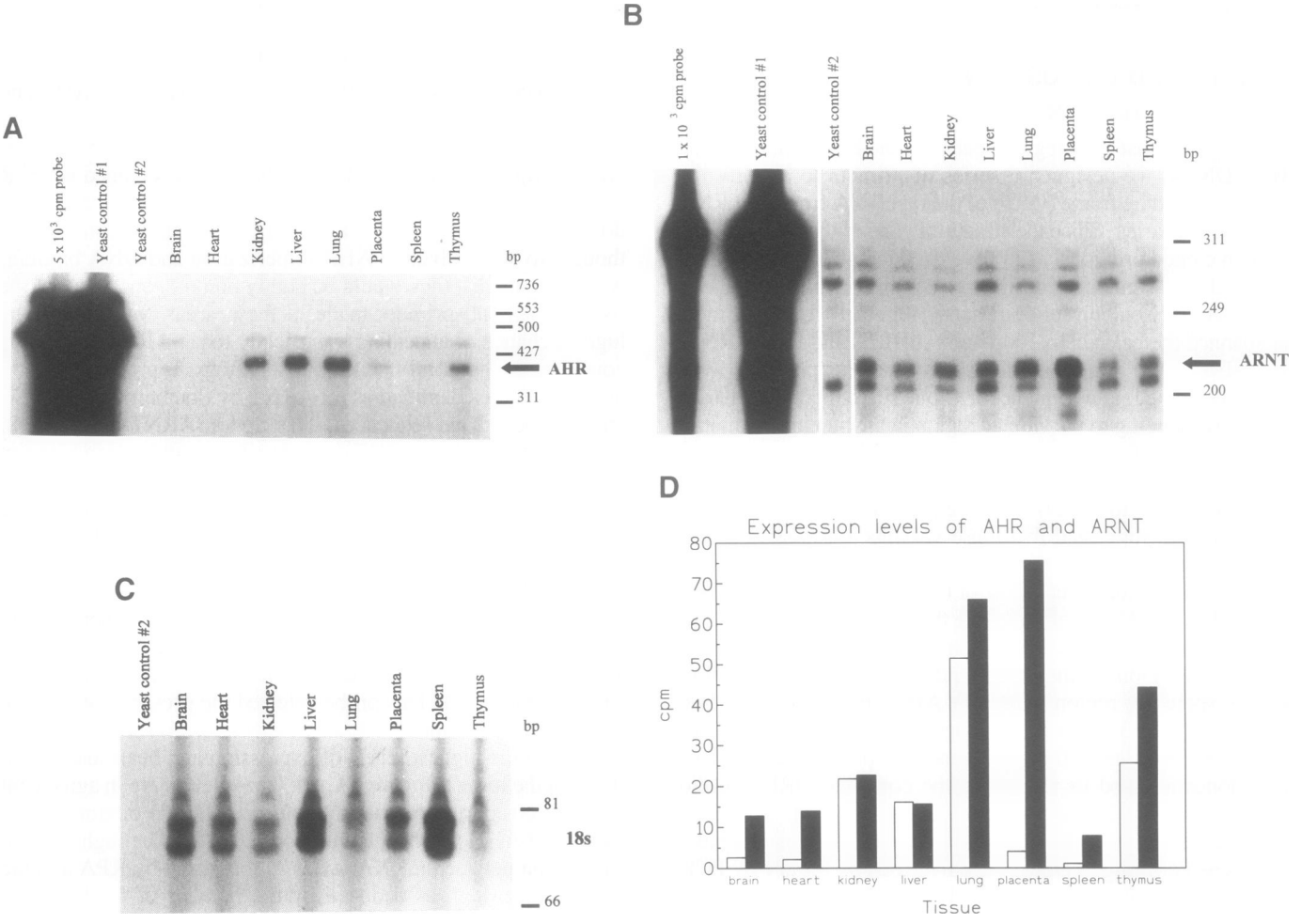

Figure 3. Ribonuclease protection analysis of the rat AHR. Each lane contains 5 μg total RNA from the indicated rat tissues. Lane marked 'probe' indicates where 5×10^3 cpm or 1×10^3 cpm of riboprobe was loaded onto the gel. Yeast control #1 and yeast control #2 lanes contain 5 μg yeast total RNA undigested or digested with the ribonucleases, respectively. **A.** Rat total RNA was probed with 1×10^4 cpm of a 419 bp riboprobe made to the *Spe*I fragment of pr32. **B.** The same tissues were probed with 5×10^4 cpm of a 224 bp riboprobe made from the *Sac*I fragment of rARNT-bHLH/PAS. The arrow indicates specific ARNT protected fragment in these tissues. The additional bands represent non-specific hybridization since they are also found in the yeast control #2 negative control lane. **C.** 5 μg of each total RNA was hybridized with an 80 bp riboprobe made to a highly conserved region of the human 18S ribosomal RNA cDNA (pT7 RNA 18S, Ambion Inc., Austin TX). The 80 nucleotide protected fragment will sometimes runs as a doublet, therefore, both major bands represent 18S RNA (Ambion product literature). The bands were quantitated on a Fuji BAS 2000 Phosphoimager and the relative intensities of the AHR bands in phosphoimager units (normalized to the intensities of the corresponding 18S bands) are as follows: brain, 67; heart, 46; kidney, 556; liver, 405; lung, 1347; placenta, 121; spleen, 27; thymus, 675. The relative intensities of the ARNT bands are brain, 43; heart, 46; kidney, 76; liver, 52; lung, 220; placenta, 252; spleen, 26; thymus, 148. D. Histogram showing the relative expression of AHR and ARNT across tissues. The relative intensities of the AHR and ARNT mRNAs were quantitated as described above, normalized to the corresponding 18S bands, and phosphoimager units converted to cpms. The white bars depict AHR levels while the black bars indicate ARNT levels.

all tissues with placenta, lung, and thymus containing the highest levels and spleen, brain, and heart containing the lowest (Figure 3B, C). Surprisingly, the one tissue where a large difference in AHR/ARNT expression was detected was in placenta. This tissue appeared to have very low levels of AHR compared to ARNT mRNA. The fact that ARNT appears to be expressed in such large excess over the AHR may indicate an additional physiological role for ARNT in this tissue at this gestational time point (see discussion above).

Functional expression of the rat AHR cDNA

Both the full length and splice variant of the rat AHR cDNAs were expressed and *in vitro* labelled with [^{35}S]methionine using a rabbit reticulocyte lysate system (24). Although the calculated molecular weight of the rAHR and rAHR/Δ142−376 are 96 kD and 70 kD respectively, SDS-PAGE analysis revealed products of approximately 106 kD and 66 kD (Figure 4A). This difference between the calculated size and the mobility of the protein has been observed previously for both the mouse and human AHR and is presumably due to anomalous migration on SDS-PAGE or to post-translational modifications of the proteins (26,27). To analyze the expressed rAHR's ability to bind to the DRE sequence, *in vitro* translated product and oligonucleotides containing the DRE were used in gel shift assays (Figure 4C). As expected, the AHR was able to bind the DRE in the presence of the dimeric partner ARNT in an agonist dependent manner. To test for ligand binding activity, we photoaffinity labelled the *in vitro* expressed rAHR with the photoaffinity ligand 2-azido-3-[^{125}I] iodo-7,8-dibromodibenzo-*p*-dioxin (generous gift of Alan Poland, McArdle Laboratory, Madison, Wis.)(Figure 4B). We observed that the labelled product exhibited a mobility of about 106 kD upon SDS-PAGE which is consistent with the previously reported mobility of an allele of the Fisher 344 rat photoaffinity ligand binding was able to be displaced by excess AHR (17). Further, this interaction was specific as the amounts of β-naphthaflavone (βNF), another agonist of the AHR.

Despite its apparent low level of expression, we were interested in characterizing the biochemical properties of the splice variant, rAHR/Δ142−376. This variant intrigued us because it has a deletion of almost the entire PAS domain while maintaining an ORF from the consensus initiation methionine through the AHR stop codon. Since this molecule retained the bHLH domain but lacked sequences involved in ligand binding, we questioned whether this species might weakly dimerize with ARNT and thus bind DREs independent of agonist. In contrast to the full length receptor, rAHR/Δ142−376 did not bind to the DRE in gel shift assays (in the presence of ARNT) (Figure 4C) nor did it show any ligand binding activity (Figure 4B). Although these results coupled with the RPA suggest that this variant probably has little *in vivo* significance, it does provide support for our previous receptor domain structure and modeling studies (24). First, even though the splice variant contains an intact bHLH domain, a deletion of most of the PAS domain results in a protein that does not dimerize with ARNT to form DRE binding complexes (Figure 4C). This observation supports the idea that the PAS domain contains sequences that are involved in AHR-ARNT interactions and are required for dimerization between these molecules. In addition, the observation that the variant does not bind ligand (Figure 4B) is in agreement with our previous findings that exons 7 and 8 encode sequences that form the ligand binding pocket of the AHR. Although it cannot be ruled out that these negative results are due to improper folding of this variant protein, our recent results with a variety of deletions and chimeric molecules suggests that the domains involved in ligand binding, DRE binding, Hsp90 association and transcriptional activation have the potential to function independently and in a variety of different contexts (our unpublished observations) (24).

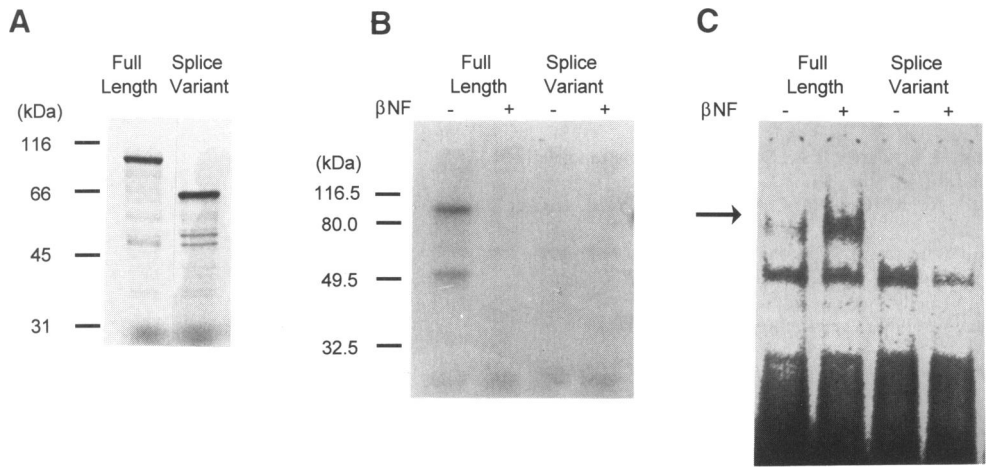

Figure 4. Functional analysis of the AHR and splice variant. **A.** *In vitro* expression of prAHR and prAHR/Δ142−376. Rabbit reticulocyte lysate expressed AHRs were labelled with [^{35}S]methionine and analyzed by 7.5% PAGE. The rAHR and rAHR/Δ142−376 cDNAs produced proteins of 106 kDa and 66 kDa respectively. **B.** Photoaffinity labelling of AHR. The rat full length receptor and the splice variant were expressed by *in vitro* transcription/translation, photoaffinity labelled with 2-azido-3[^{125}I]iodo-7,8-dibromodibenzo-*p*-dioxin and electrophoresed on a 10% polyacrylamide gel. Ligand binding specificity was demonstrated by competition with 100 nM βNF. **C.** Gel shift analysis demonstrating binding of AHR-ARNT heterodimers to the DREs. 5 μl of rabbit reticulocyte lysate expressing full length rat AHR or the splice variant were incubated with 5 μl of rabbit reticulocyte lysate expressing human ARNT for 2 hours at 30°C the presence or absence of 100 μM βNF. This complex was then incubated at room temperature with poly dIdC then with ^{32}P-end labelled DREs followed by PAGE analysis. The gel was exposed to Fuji phosphoimaging plates for 12 hours and subsequently developed on a Fuji BAS2000 Phosphoimager. The image was analyzed using the Photofinish program (v.1, Zsoft Corporation) using the following equalization settings: 0 low, 127 mid, and 255 high. A Polaroid photo was taken of the screen for output.

ACKNOWLEDGEMENTS

This work was supported by the Pew Foundation, The American Cancer Society (JFRA-303) and the National Institutes of Health (ES-5703 and T32-GM08061).

REFERENCES

1. Poland, A. and Knutson, J.C. (1982) *Ann. Rev. Pharmacol. Toxicol.*, 22, 517–554.
2. Nebert, D.W. and Gonzalez, F.J. (1987) *Ann. Rev. Biochem.*, 56, 945–993.
3. Nebert, D.W. and Gelboin, H.V. (1969) *Arch. Biochem. Biophys.*, 134, 76–89.
4. Safe, S. (1990) *Crit. Rev. Toxicol.*, 21, 51–88.
5. Gielen, J.E., Goujon, F.M. and Nebert, D.W. (1972) *J. Biol. Chem.*, 247, 1125–1137.
6. Poland, A., Glover, E. and Kende, A.S. (1976) *J. Biol. Chem.*, 251, 4936–4946.
7. Poland, A. and Glover, E. (1980) *Mol. Pharm.*, 17, 86–94.
8. Swanson, H.I. and Bradfield, C.A. (1993) *Pharmacogenetics*, 3, 213–230.
9. Greenlee, W.F.and Poland, A. (1979) *J. Biol. Chem.*, 254, 9814–9821.
10. Pollenz, R.S., Sattler, C.A. and Poland, A. (1994) *Mol. Pharm.*, 45, 428–438.
11. Perdew, G.H. (1988) *J. Biol. Chem.*, 263, 13802–13805.
12. Hoffman, E.C., *et al.* (1991) *Science*, 252, 954–8.
13. Telakowski-Hopkins, C.A., King, R.G. and Pickett, C.B. (1988) *Proc. Natl. Acad. Sci. USA*, 85, 1000–1004.
14. Neuhold, L.A., Shirayoshi, Y., Ozato, K., Jones, J.E., and Nebert, D.W. (1989) *Mol. Cell. Biol.*, 9, 2378–86.
15. Shen, E.S. and Whitlock, J.S., Jr. (1992) *J. Biol. Chem.*, 267, 6815–6819.
16. Fujisawa-Sehara, A., Yamane, M., Kuriyama, Y. (1988) *Proc. Natl. Acad. Sci. USA*, 85, 5859–5863.
17. Poland, A., and Glover, E. (1987) *Biochem. Biophys. Res. Comm.*, 146, 1439–1449.
18. Swanson, H.I. and Perdew, G.P. (1991) *Tox. Lett.*, 58, 85–95.
19. Denison, M.S., Phelps, C.L., Dehoog, J., Kim, H.J., Bank, P.A., and Yao, E.F., in Biological Basis of Risk Assessment of Dioxins and Related Compounds. 1991, Cold Spring Harbor Press: Cold Spring Harbor. p. 337–350.
20. Gasiewicz, T.A. and Rucci, G. (1984) *Mol. Pharm.*, 26, 90–98.
21. Sanger, F., Nicklen, S. and Coulson, A.R. (1977) *Proc. Natl. Acad. Sci. USA*, 74, 5463–5467.
22. Melton, D.A., Krieg, P.A., Rebegliati, M.R., Maniatis, T., Zinn, K., and Green, M.R. (1984) *Nucl. Acids Res.*, 12, 7035–7056.
23. Hod, Y. (1992) *BioTechniques*, 13, 852–853.
24. Dolwick, K.M., Swanson, H.I. and Bradfield, C.A. (1993) *Proc. Natl. Acad. Sci. USA*, 90, 8566–8570.
25. Schmidt, J.V., Carver, L.A. and Bradfield, C.A. (1993) *J. Biol. Chem.*, 268, 22203–2209.
26. Dolwick, K.M., Schmidt, J.V., Carver L.A., Swanson, H.I., and Bradfield, C.A. (1993) *Mol. Pharm.*, 44, 911–917.
27. Burbach, K.M., Poland, A. and Bradfield, C.A. (1992) *Proc. Natl. Acad. Sci. USA*, 89, 8185–8189.
28. Ema, M., Sogawa, K., Watanabe, N., Chujoh, Y., Matsushita, N., Gotoh, O., Funae, Y., Fujii-Kuriyama, Y. (1992) *Biochem. Biophys. Res. Comm.*, 184, 246–253.
29. Myers, E.W. and Miller, W. (1988) *Computer Applications in the Biosciences*, 4, 11–7.
30. Whitelaw, M.L., Gottlicher, M., Gustafsson, J-A., Poellenger, L. (1993) *EMBO J.*, 12, 4169–4179.
31. Huang, Z.J., Edery, I. and Rosbash, M. (1993) *Nature*, 364, 259–262.
32. Carlstedt-Duke, J.M.B. (1979) *Cancer Res.*, 39, 3172–3176.